Aerosol Science and Technology

ISSN: (Print) (Online) Journal homepage: https://www.tandfonline.com/loi/uast20

# Quantification of cooking organic aerosol in the indoor environment using aerodyne aerosol mass spectrometers

**Erin F. Katz, Hongyu Guo, Pedro Campuzano-Jost, Douglas A. Day, Wyatt L. Brown, Erin Boedicker, Matson Pothier, David M. Lunderberg, Sameer Patel, Kanan Patel, Patrick L. Hayes, Anita Avery, Lea Hildebrandt Ruiz, Allen H. Goldstein, Marina E. Vance, Delphine K. Farmer, Jose L. Jimenez & Peter F. DeCarlo**

**To cite this article:** Erin F. Katz, Hongyu Guo, Pedro Campuzano-Jost, Douglas A. Day, Wyatt L. Brown, Erin Boedicker, Matson Pothier, David M. Lunderberg, Sameer Patel, Kanan Patel, Patrick L. Hayes, Anita Avery, Lea Hildebrandt Ruiz, Allen H. Goldstein, Marina E. Vance, Delphine K. Farmer, Jose L. Jimenez & Peter F. DeCarlo (2021) Quantification of cooking organic aerosol in the indoor environment using aerodyne aerosol mass spectrometers, Aerosol Science and Technology, 55:10, 1099-1114, DOI: 10.1080/02786826.2021.1931013

**To link to this article:** https://doi.org/10.1080/02786826.2021.1931013

AEROSOL SCIENCE AND TECHNOLOGY
2021, VOL. 55, NO. 10, 1099–1114
https://doi.org/10.1080/02786826.2021.1931013



# Quantification of cooking organic aerosol in the indoor environment using aerodyne aerosol mass spectrometers

Erin F. Katz[a,b], Hongyu Guo[c], Pedro Campuzano-Jost[c], Douglas A. Day[c], Wyatt L. Brown[c], Erin Boedicker[d], Matson Pothier[d], David M. Lunderberg[a,b], Sameer Patel[e]*, Kanan Patel[f], Patrick L. Hayes[g], Anita Avery[h], Lea Hildebrandt Ruiz[f], Allen H. Goldstein[b,i], Marina E. Vance[e], Delphine K. Farmer[d], Jose L. Jimenez[c], and Peter F. DeCarlo[j]

[a]Department of Chemistry, University of California at Berkeley, Berkeley, California, USA; [b]Department of Environmental Science, Policy, and Management, University of California at Berkeley, Berkeley, California, USA; [c]Department of Chemistry & CIRES, University of Colorado at Boulder, Boulder, Colorado, USA; [d]Department of Chemistry, Colorado State University, Fort Collins, Colorado, USA; [e]Department of Engineering, University of Colorado at Boulder, Boulder, Colorado, USA; [f]McKetta Department of Chemical Engineering, University of Texas at Austin, Austin, Texas, USA; [g]Department of Chemistry, Université de Montréal, Montréal, Quebec, Canada; [h]Center for Aerosol and Cloud Chemistry, Aerodyne Research Inc, Billerica, Massachusetts, USA; [i]Department of Civil and Environmental Engineering, University of California at Berkeley, Berkeley, California, USA; [j]Department of Environmental Health and Engineering, Johns Hopkins University, Baltimore, Maryland, USA

**ABSTRACT**

The Aerodyne aerosol mass spectrometer (AMS) is used extensively to study the composition of non-refractory submicron aerosol composition during atmospheric field studies. During two recent studies of indoor environments, HOMEChem and ATHLETIC, the default ambient organic aerosol AMS quantification parameters resulted in a large discrepancy with co-located instruments while sampling cooking organic aerosol (COA). Instruments agreed within uncertainty estimates during all other sampling periods. Assuming a collection efficiency (*CE*) of unity, adjustments to the AMS relative ionization efficiency (*RIE*) were required to reach agreement with co-located instruments. The range of $RIE_{COA}$ observed (ATHLETIC: $RIE_{COA} = 4.26–4.96$, HOMEChem: $RIE_{COA} = 4.70–6.50$) was consistent with *RIE* measured in the laboratory for cooking-specific molecules. These results agree with prior AMS studies which have indicated that more oxidized outdoor ambient organic aerosol has a relatively constant *RIE* of $1.4 \pm 0.3$ while more reduced organics have higher *RIE*. The applicability of a higher *RIE* was considered for two ambient datasets, and agreement between the AMS and co-located instruments improved when an increased response factor ($RIE \times CE$) was applied to positive matrix factorization-derived primary organic aerosol (POA). Based on the observations presented here and the literature, we recommend AMS users consider applying $RIE_{COA}$=4.2 to source and indoor studies of COA and evaluate a higher POA response factor of the order of ~1.5 in outdoor studies at urban background sites, and ~2 at sites impacted by fresh sources. This study aims to improve AMS quantification methodology for reduced POA and highlights the importance of careful intercomparisons in field studies.

**ARTICLE HISTORY**
Received 16 February 2021
Accepted 6 May 2021

**EDITOR**
Jim Smith

## 1. Introduction

Recently, there has been an increased focus on chemistry occurring in the indoor environment, with advanced instrumentation typically employed in outdoor atmospheric chemistry studies being used indoors (Nazaroff and Goldstein 2015; Farmer et al. 2019; Abbatt and Wang 2020). This interest in the indoor environment is motivated by the fact that humans, especially in developed nations, spend most of their time indoors (Klepeis et al. 2001). To accurately assess human exposure and health risks associated with particulate matter, it is essential to understand aerosol sources and dynamics in the home and other indoor spaces.

The Aerodyne aerosol mass spectrometer (AMS) is a widely used instrument for the quantitative study of ambient submicron particulate matter ($PM_1$, aerosols with aerodynamic diameter $\leq 1\,\mu m$) at high time

**CONTACT** Peter F. DeCarlo pdecarl1@jhu.edu Department of Environmental Health and Engineering, Johns Hopkins University, Baltimore, MD, USA.
*Current affiliation: Indian Institute of Technology Gandhinagar, Palaj, Gandhinagar, Gurjat, India

Supplemental data for this article is available online at https://doi.org/10.1080/02786826.2021.1931013.

resolution (DeCarlo et al. 2006; Canagaratna et al. 2007; Guo et al. 2020). Detection of aerosols using the AMS involves thermal vaporization and electron ionization leading to fragmentation of the molecules found in particles. Species typically quantified by the AMS include those that vaporize in a few seconds at 600 °C ("non-refractory species"). Particulate sulfate ($SO_4$), nitrate ($NO_3$), ammonium ($NH_4$), organics (OA), and non-refractory chloride (Chl) are quantified following standard methodology, while black carbon and dust are not (Allan et al. 2003). The AMS is also capable of measuring the size distribution of non-refractory $PM_1$ with chemical speciation. The size range of the AMS (~50 nm to ~750 nm in vacuum aerodynamic diameter for 50% transmission) is relevant for human exposure, cloud formation, and urban air quality, to name a few (Canagaratna et al. 2007; Hu et al. 2017; Guo et al. 2020).

The high level of fragmentation via combined thermal vaporization and electron ionization in the AMS detection scheme makes identification and quantification of specific organic parent molecules difficult. Bulk OA is quantified in the AMS based on laboratory calibrations (Slowik et al. 2004; Canagaratna et al. 2007; Dzepina et al. 2007; Jimenez et al. 2016; Robinson et al. 2017; Xu et al. 2018) which have reported an average relative ionization efficiency (*RIE*) of ~1.4 relative to nitrate, the primary calibrant. This parameter has been proven robust and accurate within uncertainties in ambient aerosol studies (Canagaratna et al. 2007; Jimenez et al. 2016; Guo et al. 2020; Hu et al. 2020). The possibility that chemically reduced OA could have a higher response factor in the AMS was first suggested by Jimenez et al. (2003), who considered the larger electron ionization cross section of reduced versus oxidized molecules. Exploring this effect in some ambient studies indicated a limited impact on the response (at most +50%) for reduced versus oxidized aerosols (Docherty et al. 2011; Jimenez et al. 2016). Pinpointing the discrepancies caused by reduced OA has been difficult due to the ambient mixture of reduced OA present and a usually higher fraction of more oxidized OA, especially secondary OA (SOA), in most ambient studies (e.g., Zhang et al. 2007). The typically minor fraction of primary OA (POA) in many studies also led to less focus on reduced POA in subsequent AMS studies in general. Jimenez et al. (2016) and Xu et al. (2018) recently reported higher *RIE* values for very reduced pure-component species in the laboratory, which need to be taken into consideration for laboratory studies using pure OA compounds. Murphy (2016) proposed an AMS detection model that suggested reduced species, which undergo less fragmentation, may be detected with higher *RIE* due to higher molecular weight species having longer dwell times in the detection region. Although the general physical phenomenon is likely to play a role in overall AMS sensitivity, the specific mathematical model of Murphy (2016) has been shown to be inconsistent with observations (Jimenez et al. 2016; Hu et al. 2017; Ide, Uchida, and Takegawa 2019; Uchida, Ide, and Takegawa 2019). Additional complex processes must occur in the AMS detection scheme, but so far, theoretical models have not been able to successfully reproduce observed AMS detection properties (Jimenez et al. 2016; Xu et al. 2018; Ide, Uchida, and Takegawa 2019).

Cooking is a source of POA in outdoor and indoor environments. During cooking, particle mass can originate from the food itself and from combustion sources used to cook food. Field and laboratory studies have shown that cooking organic aerosol (COA) is largely comprised of chemically reduced components, such as fatty acids (e.g., oleic acid, stearic acid, palmitic acid, others), in addition to glycerides, sugars, and anhydrous sugars (Abdullahi, Delgado-Saborit, and Harrison 2013). Factor analysis (typically through positive matrix factorization, PMF) is widely employed in AMS outdoor analyses to separate different OA sources (Lanz et al. 2007; Ulbrich et al. 2009). Urban studies involving the AMS have attributed ~5–20% of the measured ambient aerosol mass to COA using PMF (Mohr et al. 2012; Crippa et al. 2013; Hayes et al. 2013; Kim, Zhang, and Heo 2018; Avery, Waring, and DeCarlo 2019). COA has been challenging to identify in the bulk UMR AMS aerosol mass spectrum using PMF because of its spectral similarity to other POA sources (e.g., vehicle emissions) (Mohr et al. 2009; Mohr et al. 2012). Studies that successfully identified COA in the bulk organic mass spectrum were close to strong, temporally trending sources (Mohr et al. 2012; Robinson et al. 2018). Reyes-Villegas et al. (2018) analyzed laboratory COA with an AMS and reported high response factors (1.56 to 3.06) compared to the value used for ambient OA (1.4). Using this data, the authors suggested that the discrepancy published by Yin et al. (2015) between AMS-PMF-derived COA and filter-based chemical mass balance (CMB)-derived COA could be caused by the COA response factor in the AMS. Minguillón et al. (2015) also presented a disagreement between ambient Aerosol Chemical Speciation Monitor (ACSM; a smaller, lower cost, and simpler to operate versions of AMS, described in Ng et al. 2011) organic

concentrations and filter-based measurements, possibly due to a high ACSM response factor, but did not resolve the discrepancy. Docherty et al. (2011) and Jimenez et al. (2016) characterized quantification discrepancies caused by ambient POA and found that a combined response factor ($RIE \times CE$, collection efficiency) of 1.5, at the lower end of the Reyes-Villegas laboratory derived factor, could improve the agreement between AMS and co-located instruments.

Two recent comprehensive field studies, HOMEChem (House Observations of Microbial and Environmental Chemistry) and ATHLETIC (Athletic center study of Indoor Chemistry), involved the study of indoor air in two environments: a residential test house and a university athletic center. The HR-AMS involved in each campaign was unique and independently operated. Intercomparisons between the calculated AMS volume and co-located particle sizers revealed a large disagreement during cooking events if default outdoor ambient quantification parameters were applied to the AMS data. The AMS and co-located instruments showed agreement within error estimates during all other sampling periods. In this article, we aim to constrain the COA response factor by examining factors which contributed to the discrepancy in particle mass concentration when COA was sampled indoors. We utilize laboratory calibrations of COA-proxy molecules (e.g., oleic acid and linoleic acid) to corroborate the response factors observed in the field. Finally, we reevaluate the intercomparisons from two prior outdoor ambient field studies to determine if a higher POA response factor is applicable. We conclude by recommending methods for AMS users to address this discrepancy in future studies.

## 2. Materials and methods

### 2.1. High-resolution aerosol mass spectrometry: Instrument description

The high-resolution aerosol mass spectrometer (HR-AMS) is detailed in numerous previous studies and briefly summarized here (DeCarlo et al. 2006; Canagaratna et al. 2007). The AMS measures size-resolved $PM_1$ chemical composition for non-refractory aerosol species (organics, nitrate, sulfate, ammonium, and chloride). In the HR-AMS, submicron particles are focused into vacuum to a narrow beam by an aerodynamic lens and subsequently impact a porous tungsten surface heated to ~600 °C. The resulting vapors are ionized by 70 eV electron ionization, leading to typically small ion fragments which are periodically extracted and analyzed by a time-of-flight mass spectrometer. Particle size distributions can be derived by recording the instrument signal as a function of the particles' time-of-flight (PToF) through the vacuum chamber prior to impaction on the heated surface.

### 2.2. Aerosol mass spectrometry: Quantification theory and background

In order to provide necessary context for the relative ionization efficiency (*RIE*) determinations, here we review the quantification methodology for AMS. The raw ion rate output of the AMS is converted to a mass concentration according to Equation (1) (Canagaratna et al. 2007).

$$C_s = \frac{10^{12}\ MW_{NO3}}{CE_s\ RIE_s\ IE_{NO3}\ Q\ N_A} \sum_{all\ i} I_{s,i} \tag{1}$$

Ion rates at all $i$ $m/z$ corresponding to a given species $s$, $I_{s,i}$, are summed and converted to mass concentration, $C_s$. $10^{12}$ is a conversion factor to the units of μg/m$^3$, $Q$ is the flow rate, $N_A$ is Avogadro's number, and $MW_{NO3}$ is the molecular weight of nitrate, the primary calibrant. The remaining parameters, $CE_s$ (collection efficiency of species, s), $IE_{NO3}$ (ionization efficiency of nitrate), and $RIE_s$ (relative ionization efficiency of species, s, compared to nitrate) directly relate to quantification of a species of interest, $s$, and are based on calibrations and/or empirical parameterizations.

Nitrate is the primary calibrant for the AMS because it is common in ambient aerosol, and laboratory-generated $NH_4NO_3$ aerosols are focused efficiently by the aerodynamic lens and vaporize rapidly on the AMS tungsten vaporizer without bounce, which makes it also suitable for calibrating with single particle methods. This species also leaves no background signal that may introduce noise in later measurements. Additionally, $NH_4NO_3$ has consistent and known fragmentation products with ~90% of the nitrate signal at $m/z$ 30 ($NO^+$) and 46 ($NO_2^+$) (Allan, Bower et al. 2004; Hogrefe et al. 2004; Canagaratna et al. 2007). All other species quantified by the AMS are given a relative ionization efficiency, $RIE_s$, which quantifies the differences in ions detected per molecule vaporized, compared to nitrate (Alfarra et al. 2004). Equation (2) displays how $RIE_s$ can be calculated from a species' measured ionization efficiency, $IE_s$, and molecular weight, $MW_s$.

$$RIE_s = \frac{IE_s}{MW_s} * \frac{MW_{NO3}}{IE_{NO3}} * RIE_{NO3} \tag{2}$$

$CE_s$ is the collection efficiency of the species of interest. Allan, Delia et al. (2004) first suggested using

a *CE* of 0.5 because the AMS was consistently measuring ~1/2 the submicron aerosol mass of co-located instruments. This discrepancy is mostly explained by solid or dry particles bouncing off the tungsten heater, while liquid particles are detected at higher efficiency (Allan, Bower et al. 2004; Huffman et al. 2005; Matthew, Middlebrook, and Onasch 2008). Middlebrook et al. (2012) proposed a parameterization for *CE* of ambient particles based on the fraction of ammonium nitrate and acidic sulfate in the particle phase, as proxies for phase state. Application of the Middlebrook *CE* parameterization is common today, and typically results in more accurate and robust mass quantification than applying a constant *CE* of 0.5 (Hu et al. 2017; Guo et al. 2020; Hu et al. 2020). In this study, a $2\sigma$ uncertainty of 35% is assumed for total AMS concentrations when comparing to other instrumentation, though uncertainties are higher for individual species (38% for organics, 36% for sulfate (or 34% if sulfate is calibrated in-field), and 34% for ammonium and nitrate (Bahreini et al. 2009). Most of the uncertainty (30%) is from *CE* (Bahreini et al. 2009).

### 2.3. HOMEChem field campaign

The HOMEChem study took place at the UT Austin Test House, or "UTest House" on the J.J. Pickle Research Campus in Austin, Texas, USA. The indoor air exchange rate with outdoors was $\sim 0.5 \pm 0.1\ hr^{-1}$, and the indoor recirculation rate was $8\ hr^{-1}$ (Farmer et al. 2019). Ceiling fans were constantly run to promote mixing in addition to the indoor recirculation within the main dwelling space, and the air conditioning system was set to a constant temperature of 25 °C for the experiments described in this article. Numerous cooking experiments took place throughout the HOMEChem campaign: vegetable stir-fry, breakfast, beef chili, lasagna, and Thanksgiving dinner. The ventilation hood above the stove was not operated to enable focus on the emissions of indoor cooking as opposed to effectiveness of ventilation. See Farmer et al. (2019) for more details regarding the UTest House conditions and experiments during HOMEChem.

At HOMEChem, instruments were either located inside of the UTest House kitchen or a trailer adjacent to the UTest house with insulated inlets to the kitchen. Table S1 describes all HOMEChem instruments used in this analysis, the particle size range analyzed, the type of diameter measured, and instrument location. All intercomparisons discussed in the following text with the HR-AMS involves instruments housed in the instrument trailer as opposed to the UTest House kitchen so that sampling point and inlet losses would be similar and not confound the intercomparison. However, inlet losses were expected to be minimal in the size range of interest (Figure S1). The HR-AMS inlet included an automatic valve-switching system that alternated between outdoor (5 min) and indoor (25 min) sampling. Details regarding the HR-AMS inlet, in field calibrations, and co-located instruments used for intercomparisons are in the online supplementri information (SI) Section 1.2. An ultra-high sensitivity aerosol spectrometer (UHSAS, Droplet Measurement Technologies, Boulder, CO, USA) and scanning mobility particle sizing instrument (SMPS Model 3936, comprised of a TSI 3081 long differential mobility analyzer and a TSI 3775 condensation particle counter) were used for main text intercomparisons. UHSAS saturation was observed during some experiments with exceptionally high number concentrations below 240 nm, as described in SI Section 1.3. An Aethalometer (Model AE-33, Magee Scientific Co., Berkeley, CA, USA) was used for black carbon (BC) measurements. Additional intercomparisons with SMPSs, ACSMs, and a scanning electrical mobility (particle size) spectrometer (SEMS, Brechtel Manufacturing Inc.) are shown in the SI.

### 2.4. ATHLETIC field campaign

The ATHLETIC study was conducted at Dal Ward Athletic Center, University of Colorado (CU) Boulder between November 3 and 20, 2018. A suite of instruments was installed and operated on the 2nd floor balcony of the weight room within the building to monitor the indoor air. A shared inlet with an automatic valve system switched sampling between room air and supply air every 5 min. The supply air was produced by mixing outdoor air flow and returned air flow (i.e., indoor air) at variable proportions in a large air handling unit (AHU) that serviced most of the building. The mixed outside air fraction at the main AHU flow varied from ~10–80% during this study. Temperature was maintained in the weight room at ~20 °C through a combination of conditioning at the main AHU and the local variable air volume AHU. The volume of the weight room was $1700\ m^3$ with a constant supply air flow rate of $200\ m^3$/min, resulting in a residence time of 8.5 min (Finewax et al. 2021). The instruments sampled with periodic switching between the well mixed room air and the supply air to allow for investigating the differences between the two. Regular athletic training and cleaning were performed in the weight room.

Unlike the designed cooking events sampled during HOMEChem, the cooking aerosols sampled during the ATHLETIC study were not planned and were rather ingested into the building via the active air intake from outdoor sources. The most likely source is open air barbeques on campus (Dal Ward is located right next to the CU football stadium and Nov. 16 was the day before a home game), but nearby campus dining facilities may also have contributed.

The HR-AMS and a SMPS were used to constrain the *RIE* of COA at ATHLETIC. Both instruments shared the same inlet behind the switching valve system. The details of this HR-AMS setup and operations have been discussed in Nault et al. (2018), Schroder et al. (2018), Guo et al. (2020), and specific details for this study are in SI Section 1.2.2.

### 2.5. Calculation of HR-AMS particle mass and volume concentration

*RIE* and *CE* parameters defined in Section 2.2 were initially applied to all HR-AMS data from the HOMEChem and ATHLETIC campaigns. For HOMEChem, $RIE_{OA} = 1.4$, $RIE_{NO3} = 1.1$, $RIE_{SO4} = 1.2$, $RIE_{NH4} = 4.16$, and $RIE_{Chl} = 1.3$. For ATHLETIC, $RIE_{OA} = 1.4$, $RIE_{NO3} = 1.1$, $RIE_{SO4} = 1.57$, $RIE_{NH4} = 4.25$, and $RIE_{Chl} = 1.98$. The *RIE* for HOMEChem ammonium and ATHLETIC sulfate, ammonium, and chloride were derived from in situ calibrations of size-selected particles generated by atomizing salt solutions. HOMEChem $RIE_{SO4}$ and $RIE_{Chl}$ originate from Alfarra et al. (2004). Inorganics were <5% of the measured mass during the cooking periods of interest for both studies, thus the inorganic *RIE* are expected to play a minor role in COA quantification. *CE* for periods dominated by infiltration or ventilation of outdoor aerosols or for outdoor sampling (without strong cooking influences) was estimated according to Middlebrook et al. (2012) and applied to the data. *CE* ranged between 0.5 and 0.9 for the HOMEChem and ATHLETIC studies. During periods dominated by cooking emissions, $CE = 1$ was used for both studies based on the composition dominated by organic oils (Matthew, Middlebrook, and Onasch 2008).

For volume comparisons with SMPS, the mass concentrations of AMS species were converted to partial volumes via their densities and summed assuming volume additivity and particles were spherical. OA density was estimated from the AMS OA O/C and H/C atomic ratios (calculated using the improved method of Canagaratna et al. (2015)) and the density parameterization of Kuwata, Zorn, and Martin (2012). We discuss the application of this density parameterization to COA in Section 3. For sampling not impacted by cooking emissions, the average OA density was $1.1 \pm 0.1\ g/cm^3$ during ATHLETIC and $1.3 \pm 0.1\ g/cm^3$ during HOMEChem. A combined density of $1.75\ g/cm^3$ was applied to sulfate, nitrate, and ammonium, approximated from ammonium sulfate, ammonium bisulfate, and ammonium nitrate (Sloane et al. 1991; Stein et al. 1994; Salcedo et al. 2006). A density of $1.52\ g/cm^3$ was applied for non-refractory chloride based on ammonium chloride (Salcedo et al. 2006). For outdoor intercomparisons (HOMEChem only), black carbon was converted to volume using a density of $1.78\ g/cm^3$ (Park et al. 2004).

### 2.6. Laboratory calibrations of species ionization efficiency in the AMS

*IE* calibrations were conducted in the laboratory using the HR-AMS deployed at HOMEChem with the same settings (DeCarlo et al. 2006). Known components of cooking organic aerosol were tested: oleic acid, stearic acid, linoleic acid, and squalene (Abdullahi, Delgado-Saborit, and Harrison 2013; Lunderberg et al. 2020). The procedure described by Xu et al. (2018) was adapted. Organic species were dissolved in methanol and atomized by a TSI Inc. model 3076 constant output atomizer. Aerosols were dried using a silica diffusion dryer, mobility selected by an electrostatic classifier unit (model 3080, TSI Inc.), and then mass-selected by a centrifugal particle mass analyzer (CPMA, Cambustion Ltd.). The monodisperse output was split between the HR-AMS and a condensation particle counter (CPC). A Brechtel Inc. model 1710 mixing CPC or an Aerosol Devices Inc. MAGIC CPC was used (Hering, Spielman, and Lewis 2014). Following the calibration of each organic species, the procedure was repeated to measure the *IE* of nitrate. The *IE* of each species (in ions per molecule) was calculated as the slope of ion Hz measured by the AMS versus input molecules per second. This method was used to find the nitrate *IE* to keep methodology consistent between the organics and nitrate. The uncertainty estimated for the *RIE* of laboratory generated aerosol was 30%. Error stems from the CPMA single particle mass selection (5%), CPC particle number concentration (20%), and the flow rate into the AMS (5%). The *IE* calculated for each species is an "operational" *IE*, since $H_2O$ and CO were not directly measured, and instead were calculated using the

fragmentation table as they are for ambient sampling (Allan, Delia et al. 2004).

## 3. Results

### 3.1. Observations of cooking organic aerosol (COA) during HOMEChem and ATHLETIC studies

During HOMEChem, cooking resulted in a range of bulk $PM_1$ mass concentrations and mass spectral profiles. Vegetable stir-fry preparations resulted in enhancements of $PM_1$ concentration between ~30 and 100 μg $m^{-3}$, while Thanksgiving experiments resulted in greater enhancements (up to ~250 μg $m^{-3}$, measured by SMPS with aerosol density assumption of 1 g/$cm^3$). Patel et al. (2020) presents an overview of the observed particle concentrations and size distributions at HOMEChem. With $CE = 1$ and $RIE_{OA} = 1.4$ applied, the HR-AMS initially reported concentrations much higher than co-located instruments (Figure S3). Intercomparison with volume concentrations derived from particle sizing instruments suggested that $RIE_{OA}$ may be higher for fresh COA to reach agreement between AMS and co-located instruments.

Similarly, the AMS overestimated COA concentration during the ATHLETIC study. On a few separate occasions, the instruments sampled COA-dominant plumes transported to the weight room through the supply ducts (Figure S4). The OA mass spectrum averaged during those plumes strongly correlated with COA measured during HOMEChem (Figure S5), with characteristic COA ion ratios observed, such as $m/z$ 55/57 > 1, similar to Mohr et al. (2009), Liu et al. (2018), and others (ATHLETIC $m/z$ 55/57 = 2.79, HOMEChem $m/z$ 55/57 = 1.57). The slope of the linear regression and $R^2$ between the HOMEChem and ATHLETIC COA mass spectra are 1.06 ± 0.02 and 0.97, respectively, indicating good agreement.

### 3.2. Intercomparisons using standard AMS quantification methodology

The accuracy of the HR-AMS was evaluated by first examining the frequency distribution of the HR-AMS to SMPS ratio during cooking and non-cooking sampling. Histograms of the AMS + black carbon to SMPS particle volume ratio, (AMS + BC):SMPS, and AMS to SMPS particle volume ratio are shown for HOMEChem and ATHLETIC, respectively, in Figure 1 (BC measurement not available during ATHLETIC). Ambient quantification parameters described in Section 2.5 were applied to AMS data, i.e., $RIE_{OA} = 1.4$. The SMPS located in the instrument trailer was used for the HOMEChem intercomparison. Additional intercomparisons with the HOMEChem ACSMs, UHSAS, SEMS, and UTest House SMPSs are presented in the SI Section 2 (Table S2, Figures S6–S7). In summary, there was agreement between the AMS and co-located instruments during outdoor and indoor non-cooking sampling and over-estimation by the AMS during cooking events.

### 3.3. Parameters influencing organic aerosol quantification

Three major factors may contribute to volume disagreements during cooking-dominated periods: (1)

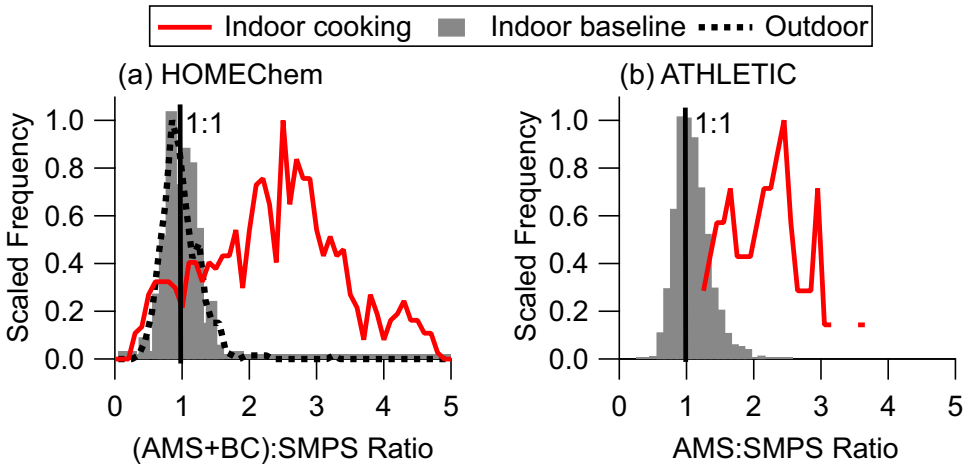


**Figure 1.** Relative frequency of (AMS + BC):SMPS or AMS:SMPS particle volume concentration ratio during outdoor, indoor baseline (non-cooking), and indoor cooking-dominated sampling periods during (a) HOMEChem and (b) ATHLETIC. HR-AMS concentration was calculated using quantification parameters for normal ambient aerosols (i.e., $RIE_{OA}$ of 1.4, see details in Section 2.5). A CE of 1.0 was applied during indoor cooking sampling and the Middlebrook et al. (2012) CE parameterization was used for indoor baseline and outdoor sampling.

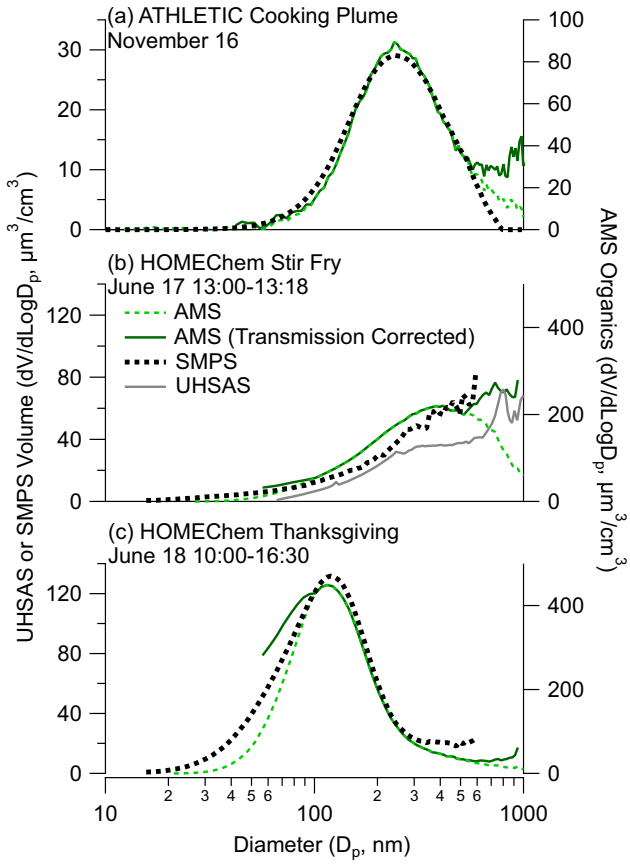


**Figure 2.** The particle volume distributions of AMS OA, SMPS, and UHSAS during (a) the ATHLETIC cooking plume on Nov. 16, (b) HOMEChem vegetable stir-fry, and (c) HOMEChem Thanksgiving 1. Density of 1.0 g/cm$^3$ was assumed for the AMS mass to volume conversion. The AMS signal is not corrected for RIE. AMS data is shown with and without transmission correction. Approximate AMS transmission curves are shown in the supplemental information.

imperfect size distribution overlap between instruments/AMS transmission efficiency variations, (2) particle density, and (3) the response factor (*RIE* and *CE*) applied to AMS data. The following discussion will demonstrate that the *RIE* and *CE* applied to AMS organic data are the most important parameters impacting the intercomparison during cooking-dominated periods, but to constrain these parameters, the first two factors must be understood.

During the ATHLETIC COA plumes and some HOMEChem experiments (Thanksgiving and breakfast), the particle size distributions were within the size range of the AMS and SMPS, and good agreement for the relative size distributions was observed (Figures 2a and c and S8b). However, during HOMEChem stir-fry and chili experiments, the size distribution was outside the size range of the SMPS (Figures 2b and S8a). The UHSAS size range extended to a diameter of 1 μm and was able to capture more of the size distribution. Because of the better size distribution overlap between AMS and UHSAS during stir-fry and chili, and saturation of the UHSAS during breakfast and Thanksgiving, we only utilize the UHSAS for intercomparison during stir-fry and chili cooking experiments.

The aerodynamic lens in the AMS has reduced transmission for particles below ~50 nm and above ~750 nm in vacuum aerodynamic diameter (Hu et al. 2017; Guo et al. 2020). Because of the particle mass observed below 100 nm during Thanksgiving and breakfast and above 600 nm during stir-fry and chili, the comparison of aerosol size distributions during HOMEChem cooking events may have been impacted by the reduced transmission efficiency of the AMS. The ATHLETIC data was minimally affected by the AMS transmission efficiency. Applying a transmission efficiency correction derived from Knote et al. (2011) and Hu et al. (2017) to the HOMEChem AMS data resulted in an average increase in integrated volume concentration of ~20% during cooking events. Without doing such a correction, the particle losses due to the AMS transmission efficiency are implicitly included in the *RIE* determinations, but we consider deviations in the transmission efficiency in the uncertainty analysis (SI Section 3), similar to previous work (Bahreini et al. 2009). Transmission corrected size distributions and transmission curves are shown in Figure S9.

Particle density can be approximated by the measured O/C and H/C ratios (Kuwata, Zorn, and Martin 2012), as described in Section 2. For the ATHLETIC COA plumes, the organic density based on O/C and H/C ratios was 0.95 g/cm$^3$. Using this method for the HOMEChem study, the average densities for Thanksgiving and stir frying were 1.0 g/cm$^3$ and 0.99 g/cm$^3$, respectively. Particle density can also be inferred by comparison of size distributions measured by AMS and SMPS. The vacuum aerodynamic diameter, $D_{va}$, measured by the AMS is related to the mobility diameter, $D_m$, measured by the SMPS and UHSAS via Equation (3) (DeCarlo et al. 2004). UHSAS optical diameters were binned to sizes which represent physical diameters of spherical particles, making them equivalent to $D_m$.

$$\frac{D_{va} * \rho_0}{\rho_p} = D_m \tag{3}$$

$\rho_0$ is unity density (1.0 g/cm$^3$), and $\rho_p$ is the particle density. The overlap in size distributions (e.g., peak centers) in Figure 3 indicates that $\rho_p \sim 1.0$ g/cm$^3$ for cooking events and therefore, that the Kuwata, Zorn,

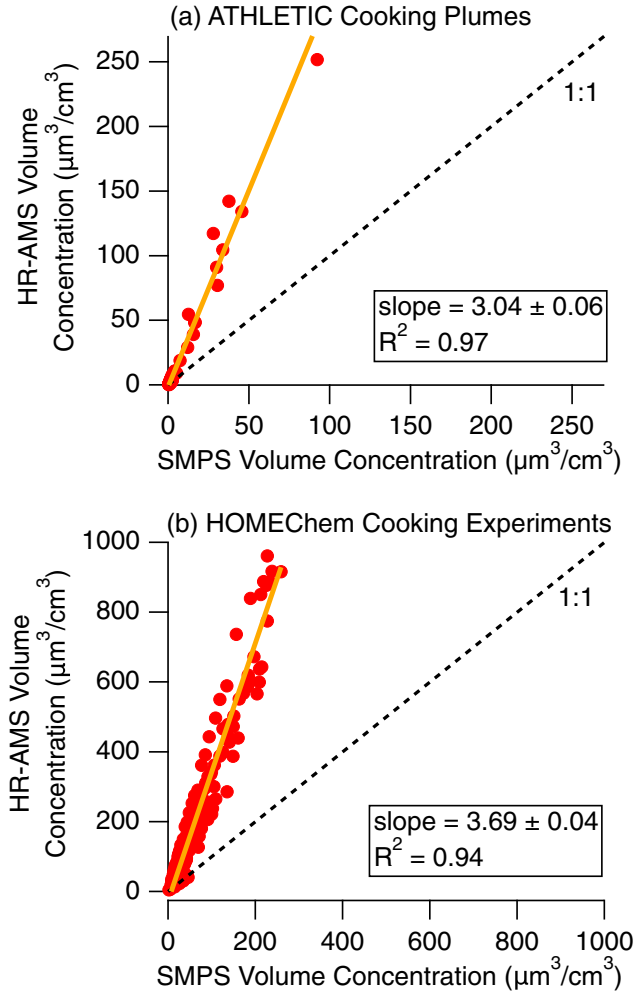


**Figure 3.** HR-AMS vs. SMPS particle volume concentration for (a) all ATHLETIC cooking plumes combined and (b) HOMEChem breakfast and Thanksgiving experiments. Thanksgiving and breakfast data are utilized because the size distributions during those experiments were within the range of SMPS sizes analyzed. AMS particle volume was calculated using $RIE_{OA}$ = 1.4, CE = 1.0, and density = 1.0 g/cm$^3$ and 0.95 g/cm$^3$ for HOMEChem and ATHLETIC, respectively. CE = 1.0 and ambient RIE and density described in Section 2.5 were applied to inorganics, though inorganics were less than 5% of the measured mass concentration. Data was fit to an orthogonal distance regression (ODR) linear fit with a non-zero y-intercept (to account for ambient OA background). The slope and $R^2$ correlation coefficient are displayed.

and Martin (2012) density parameterization is operative for fresh COA. A density of 1.0 g/cm$^3$ and 0.95 g/cm$^3$ was applied to HOMEChem and ATHLETIC cooking data, respectively, based on the Kuwata, Zorn, and Martin (2012) parameterization. The difference of up to ~5% caused by a density assumption of 1.0 g/cm$^3$ is not sufficient to explain the difference in particle loading observed during COA-influenced events at HOMEChem and ATHLETIC.

**Table 1.** RIE of cooking emissions and laboratory generated aerosol.[a]

| Cooking Emissions | RIE |
|---|---|
| Reyes-Villegas et al. (2018)* | 2.29 ± 0.47 |
| ATHLETIC Nov. 6 | 4.61 ± 1.52 |
| ATHLETIC Nov. 7 | 4.96 ± 1.64 |
| ATHLETIC Nov. 16 | 4.26 ± 1.41 |
| HOMEChem Thanksgiving | 5.73 ± 1.89 |
| HOMEChem Breakfast | 6.50 ± 2.15 |
| HOMEChem Stir Fry | 4.70 ± 1.55 |
| HOMEChem Beef Chili | 5.35 ± 1.77 |
| Three study average† | 4.16 ± 1.69 |
| *Laboratory Aerosol* | |
| Stearic Acid | 2.56 ± 0.76 |
| Oleic Acid | 3.18 ± 0.95 |
| Linoleic Acid | 5.77 ± 1.73 |
| Squalene | 6.98 ± 2.09 |
| *Laboratory Aerosol* (Xu et al. 2018) | |
| Oleic Acid | 3.0 |

[a]CE of 1.0 was assumed. The relative uncertainty ($2\sigma$) in the RIE for the ATHLETIC and HOMEChem entries shown in the table is 33% and for laboratory generated aerosols is 30% (see Sections 2 and S3). Laboratory RIE is V-mode operational.

*The *RIE* presented is an average and standard deviation of the *RIE* values reported with *CE* of 1.0. The range of *RIE* reported was 1.56 to 3.06.

†The three-study average simply takes the average of $RIE_{COA}$ from each study (HOMEChem: 5.57, ATHLETIC: 4.61, Reyes-Villegas et al. (2018): 2.29). The ± value is the standard deviation of the three $RIE_{COA}$ values, not a $2\sigma$ uncertainty.

Of the parameters discussed, the organic *RIE* and *CE* most strongly influence the calculation of HR-AMS particle concentration during cooking. When determining a source-specific *RIE*, the *CE* and *RIE* values and uncertainties are coupled if the *CE* cannot be directly measured. At HOMEChem and ATHLETIC, the *CE* was not directly measured, however, we expect the *CE* of COA to be ~1.0 because liquid aerosols have high *CE* (Matthew, Middlebrook, and Onasch 2008). For the remainder of the analysis, we assume *CE* = 1.0 during cooking. A comparison of HR-AMS particle volume versus SMPS is displayed in Figure 3 for all ATHLETIC COA plumes and HOMEChem breakfast and Thanksgiving experiments combined (experiments which showed good size distribution overlap with the SMPS). Similar plots for individual HOMEChem cooking experiments and ATHLETIC plumes are shown in Figure S10. The AMS particle volume concentration was calculated using *CE* = 1.0, $RIE_{OA}$ = 1.4 (the ambient $RIE_{OA}$), and a density of 0.95 g/cm$^3$ or 1.0 g/cm$^3$. Inorganic volume (Chl, $NO_3$, $NH_4$, $SO_4$) was calculated assuming a *CE* of 1.0 and other parameters as described in Section 2.5. The slopes in Figure 3 multiplied by 1.4 (the ambient $RIE_{OA}$) approximate the *RIE* of the bulk COA ($RIE_{COA}$), assuming the HR-AMS over-estimation during cooking is only influenced by the $RIE_{COA}$, similar to Reyes-Villegas et al. (2018). An additional correction of 1.15 (Figure S11) was applied to the HOMEChem data to account for signal above *m/z* 100 (HR masses were only fit up to *m/z* 100). Table 1 displays this estimated

$RIE_{COA}$ for HOMEChem, ATHLETIC, and laboratory generated aerosols (discussed in the next section). A comparison to values derived by Reyes-Villegas et al. (2018) is also presented (a *CE* of 1.0 was also assumed).

Inorganic volume (Chl, $NO_3$, $NH_4$) was enhanced during cooking, though it was <5% of the total mass measured by the HR-AMS during HOMEChem. Excluding inorganics from the HOMEChem volume calculation in Figure 3 resulted in less than 1% reduction in the slope, thus the $RIE_{COA}$ is not sensitive to the treatment of inorganics provided they are a small fraction of the measured mass. A similar effect was observed for black carbon, as it was usually observed at less than ~2 μg/m$^3$ during cooking unless candles were burning, so it was excluded from the calculation. Low-volatility cyclic siloxanes were detected during HOMEChem Thanksgiving experiments (Brown et al. 2021, Lunderberg et al. 2020). When siloxane ions were included in the HOMEChem organic signal (not included normally), the slope derived $RIE_{COA}$ increased by 4% assuming an *RIE* of 1.4 for siloxanes. The siloxane signals were negligible during the ATHLETIC cooking events, accounting for less than 0.1% of the total OA mass. Due to the small effect on the $RIE_{COA}$ and unknown uncertainties in their response factor in the HR-AMS, siloxanes are excluded from this analysis.

### 3.4. Laboratory calibrations of species-specific RIE

The *RIE* of pure compounds associated with cooking emissions were analyzed to validate the large $RIE_{COA}$ observed during HOMEChem and ATHLETIC. Bulk organic ion counts (measured by AMS) and particle number concentration (measured by CPC) were monitored during the calibrations. Oleic acid, stearic acid, linoleic acid, and squalene were tested. To generate the *IE* calibration curve, all organic ions (unit mass resolution) were summed and plotted versus the calculated influx of molecules per second to the AMS, derived from the DMA and CPMA single particle mobility diameter and mass and the CPC particle number concentration (Figure S12). It is likely that $CE = 1$ for oleic acid, linoleic acid, and squalene, since these were liquids at room temperature. Stearic acid was solid at room temperature, however, here we assume $CE = 1$ for consistency. If the true CE for stearic acid is less than 1.0, our reported *RIE* is biased low, which may explain why the inferred stearic acid *RIE* from our method is lower than those for the other C-18 acids. The calculated RIE values are displayed in Table 1 and have an estimated 30% uncertainty (sources of uncertainty detailed in Section 2). The mass spectrum for each species is displayed in Figure S13 with key ions noted. Our results agree well with comparable values published by Xu et al. (2018) for oleic acid. They report *RIE* of 3.0 for oleic acid using a similar experimental setup, compared to our *RIE* of $3.18 \pm 0.95$. Our range of *RIE* for HOMEChem cooking emissions (4.70 to 6.50) is within the range of *RIE* calculated for laboratory species tested on the same instrument (2.56 to 6.98). The oleic acid *RIE* was 2.0 for the ToF-ACSM. More details on the laboratory calibrations are presented in the SI Section 4.

### 3.5. Applying new quantification parameters to HOMEChem data

When applying the new *RIE* to field data, one important issue was identified: HOMEChem bulk organic mass spectra varied depending on the specific cooking activity and ingredients used. For example, during stir frying, the addition of stir fry sauce containing sugars to the hot pan immediately increased the concentration of more oxidized organic aerosol compared to when vegetables were sautéing in cooking oil (Farmer et al. 2019). Based on the findings of Xu et al. (2018), *RIE* should vary in the AMS with differences in species oxidation state. Xu et al. (2018) showed that more reduced species (e.g., oleic acid and squalene) can have a higher *RIE* and that after a certain oxidation state threshold, the *RIE* of species levels off to $1.4 \pm 0.3$. Consequently, higher *RIE* may be expected for reduced components of ambient organic aerosol, such as COA and hydrocarbon-like organic aerosol (HOA), originating from primary sources, such as vehicles. If this effect is important in a dataset, it can be approximately corrected for by separating the organic aerosol (OA) into discrete components using positive matrix factorization (PMF) (Lanz et al. 2007, Ulbrich et al. 2009) and applying different *RIE* and *CE* to individual components.

A four-factor PMF solution was chosen to describe the HOMEChem indoor HR-AMS OA mass spectral matrix during cooking. The PMF Evaluation Tool, PET, version 3.04 A software was used to conduct the PMF analysis. The SI Section 5 includes the details of the PMF analysis and the criteria to choose the final solution. The OA components during cooking include one oxidized factor ("cBBOA, or cooking-associated burning/browning OA" estimated $O/C = 0.61$) and three reduced factors ("COA1, or cooking OA 1," "COA2, or cooking OA 2," and "cHOA, or cooking-

associated HOA" with estimated O/C of 0.12, 0.16, and 0.07, respectively). The mass spectrum of each PMF factor is shown in Figure S14, and the time series of each factor's mass concentration during example cooking experiments is shown in Figure S15. Existing literature indicates that AMS quantification of ambient biomass burning OA using the standard organic *RIE* ($1.4 \pm 0.3$) is robust (Crounse et al. 2009; Aiken et al. 2010). Based on Xu et al. (2018) and these other ambient observations of biomass burning plumes, the relatively higher level of oxidation of cBBOA should merit the use of the standard organic *RIE* of 1.4. A higher *RIE* is likely only needed for the reduced factors, COA1, COA2, and cHOA.

A custom-fit function (Equation (4)) to the SMPS or UHSAS total measured volume concentration was utilized to estimate the *RIE* of the reduced COA factors while keeping fixed quantification parameters for inorganic ions ($SO_4$, $NO_3$, $NH_4$, Chl; i.e., the *RIE* described in Section 2.5 and $CE = 1$) and cBBOA ($RIE = 1.4$, density $= 1.3\ g/cm^3$ based on the Kuwata expression).

$$SMPS\ \ Volume = \frac{[SO_4]}{a} + \frac{[NO_3]}{b} + \frac{[NH_4]}{c} + \frac{[Chl]}{d} + \frac{[cBBOA]}{e} + \frac{[COA1]}{F} + \frac{[COA2]}{F} + \frac{[cHOA]}{F} \quad (4)$$

$a$, $b$, $c$, $d$, $e$, and $F$ are the effective quantification parameters for each species, $RIE \times CE$, and density for conversion to volume. $F$ was determined by the fitting the data to SMPS or UHSAS volume for each cooking experiment separately. For example, the *RIE* of the reduced COA factors was found to be 6.84 and 5.99 (using HR PMF data up to *m/z* 100 and the 1.15x correction for masses greater than *m/z* 100) for the first Thanksgiving experiment and stir fry experiments on June 17, respectively, via the custom fit method. However, it is unclear if this method ("custom fit method") is preferred (versus applying a bulk *RIE* to all factors, "bulk method") for the HOMEChem cooking dataset. When the bulk method was applied to Thanksgiving 1, the correlation between AMS and SMPS improved slightly compared to the custom fit method ($R^2 = 0.96$ versus 0.90, and slope = 0.97 versus 1.04, respectively, Figure S16). For stir fry experiments, the opposite was true. The correlation with the UHSAS was slightly worse when the bulk method was applied (Figure S16).

For ambient datasets with more diverse OA sources and more clearly resolved oxygenated factors, applying a higher *RIE* to chemically reduced PMF factors may consistently improve agreement. Overall, agreement with the SMPS was within error estimates for each method. To remain consistent with the current understanding and laboratory experiments, PMF factors will be presented with $RIE_{cBBOA} = 1.4$. Time series of PMF factors calculated with the two methods are shown in Figure S15. The time series of particle volume concentration measured by SMPS and AMS (AMS data quantified using the custom fit method) for HOMEChem Thanksgiving experiment 2 is shown in Figure 4.

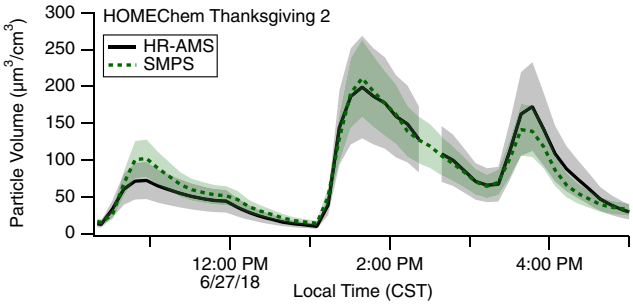


**Figure 4.** HR-AMS and SMPS particle volume concentration during HOMEChem Thanksgiving 2. HR-AMS particle volume was calculated using an RIE of 5.34 applied to COA1, COA2, and cHOA and an RIE of 1.4 (the typical ambient value) for cBBOA. CE of 1.0 was used for all species. The shading represents an uncertainty of 35% for the HR-AMS and 25% for the SMPS concentrations. The RIE of the chemically reduced PMF factors was calculated via the custom-fit method (Equation (S1)). The data shown are 10-min averages to improve agreement between the two instruments but still show high time resolution.

### 3.6. Applicability to outdoor datasets

Despite the need for a $RIE_{COA}$ correction during HOMEChem and ATHLETIC, it is unclear the extent to which ambient COA retains a high response factor, as it is greatly diluted outdoors, with evaporation and potentially retention of only less volatile material, changes in the size distribution, and chemical aging playing a role. It is possible that a potentially higher $RIE_{COA}$ has not been identified in prior ambient AMS intercomparisons because of the relatively low contribution of COA to total OA in general. For example, if COA is 20% of the total mass concentration with $RIE = 1.4$ and $CE = 0.5$, applying an updated combined response factor ($RIE \times CE$) of 4.16 would cause only a ~17% change in mass concentration, which is within the 35% uncertainty estimate for AMS total mass concentration. Once the COA or total reduced primary OA (POA) fraction exceeds ~50%, the bias due to the AMS response factor may be more obvious in intercomparisons with sizing instruments like SMPS. Indoors, where fresh COA can be a large fraction of the total aerosol mass, the discrepancy

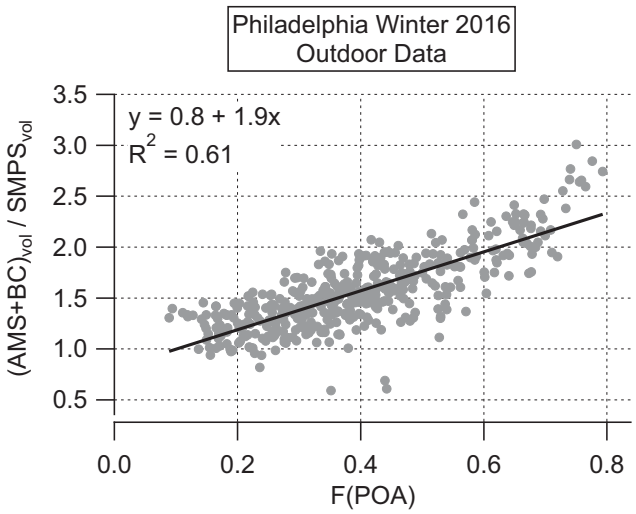


**Figure 5.** Ambient data from Avery, Waring, and DeCarlo (2019) highlighting a discrepancy between the AMS and SMPS, likely caused by a high POA response factor, or RIE × CE. The ratio of AMS + BC to SMPS volume is plotted on the y-axis versus the POA (COA + HOA) volume fraction, F(POA). All organic species are quantified using RIE = 1.4 and CE = 0.5 (typical ambient parameters). Data with the inorganic fraction >0.4 were excluded to avoid presenting confounding discrepancies not caused by POA.

caused by the AMS response factor cannot be overlooked or lumped into the general uncertainties of the technique.

Careful re-analysis of two ambient datasets, Hayes et al. (2013) and Avery, Waring, and DeCarlo (2019), suggest a higher combined response factor (*RIE* × *CE*) for POA improves agreement between the AMS and co-located instruments. The Avery, Waring, and DeCarlo (2019) winter dataset from Philadelphia, Pennsylvania 2016 showed a discrepancy between the AMS and SMPS during sampling periods with high POA mass fraction (Figure 5). Because of sampling proximity to food trucks, it is likely that fresh COA plumes were sampled frequently. Discrepancies were also identified when the POA fraction (F(POA)) was low (<0.2) and the inorganic fraction was high (>0.4), likely due to a higher actual *CE* or sulfate *RIE* (a bulk *CE* of 0.5 was used) (Figure S17). Time periods with inorganic mass fraction >0.4 were excluded from this analysis to isolate the discrepancies caused by POA, as AMS inorganic quantification and *CE* evaluation is outside the scope of this work. With ambient parameters applied to POA ($RIE_{POA}$ = 1.4 and *CE* = 0.5), the AMS to SMPS ratio increased linearly with increasing POA fraction, as shown in Figure 5. The concentration time series from periods with high F(POA) highlights how agreement with the SMPS improves when a high response factor (*RIE* × *CE*) is applied to POA (4.16 as opposed to 0.7) (Figure S18).

The Hayes et al. (2013) dataset from the 2010 CalNex campaign in Pasadena, California was likely influenced by regional COA, in contrast to fresher COA plumes sampled in Avery, Waring, and DeCarlo (2019). Our re-analysis focuses on data from Memorial Day weekend when the COA mass fraction was high and other species were observed at relatively low concentrations. Because multiple instrument issues were present, the correlation ($R^2$) between the time series of AMS organic carbon (OC) and Sunset Labs OC measurement was used to identify the range of optimal POA response factor. The $R^2$ was at a maximum when a POA response factor (*RIE* × *CE*) of ~1.5 to 2.0 was used (Figure S19), and remained within 5% of that value to higher response factors. Docherty et al. (2011) and Jimenez et al. (2016) also determined a POA response of ~1.5 was appropriate for the SOAR field campaign in Riverside, California. Similarly, the $R^2$ of the AMS versus SMPS volume for the Avery, Waring, and DeCarlo (2019) dataset was highest when *RIE* × *CE* = 1.5 was applied to POA, but remained high and the slope leveled off with increasing response factors, likely because of the impact of fresher COA in this dataset.

Together, re-analysis of these ambient datasets in contrast with fresh COA sampled indoors suggest that the AMS is most sensitive to freshly emitted COA, and by extension, possibly other POA as well. The heightened sensitivity is still present, but at a lower magnitude, for ambient POA (COA + HOA). Further analysis of additional primary aerosol sources and ambient datasets is needed to better understand the AMS response factor to chemically reduced organic aerosol during source sampling and urban and rural/remote ambient measurements.

## 4. Conclusions and discussion

Intercomparisons between the HR-AMS and co-located instruments indicated the AMS quantification parameters typically used for ambient analysis were suitable for the HOMEChem and ATHLETIC datasets during sampling periods not heavily impacted by cooking emissions. However, there was a large discrepancy during periods of sustained cooking emission influence. We found that a modified *RIE* in the range of 4.26 to 6.50 was required when COA was sampled indoors during the HOMEChem and ATHLETIC field studies, a substantial increase from the ambient organic *RIE* of 1.4 (*CE* of 1.0 was

assumed during cooking periods). The *RIE* calculated for HOMEChem and ATHLETIC data fell within the range of *RIE* calculated for laboratory generated aerosol of species expected to be in COA (e.g., oleic and linoleic acid). A $2\sigma$ uncertainty of 33% was estimated for the measurement of *RIE* for COA sampled during HOMEChem and ATHLETIC.

Considering the range of $RIE_{COA}$ presented here (4.26 to 6.50) and Reyes-Villegas et al. (2018) (1.56 to 3.06), it is possible that different cooking styles and ingredients can influence the response factor in the AMS. The *RIE* of laboratory generated oleic acid aerosols, a major decomposition product of rapeseed and olive oil, was $3.18 \pm 0.95$, while the *RIE* of linoleic acid, a major decomposition product of soybean oil, was $5.77 \pm 1.73$. The higher *RIE* observed during HOMEChem is possibly due to the use of soybean versus rapeseed oil for cooking, compared to Reyes-Villegas et al. (2018). The implications of a highly variable and elevated COA *RIE* are greatest if sampling near a strong cooking source (e.g., experiments like HOMEChem), and less significant for ambient datasets when occasional COA-dominant events are sampled (e.g., ATHLETIC). The variability in size distributions observed for different cooking experiments at HOMEChem (Figure 2), in addition to the variable *RIE*, highlights the complexity in COA detection and quantification with the AMS. It is important to constrain these variables under controlled settings to better understand the AMS response to ambient organic aerosol, especially in urban environments with numerous primary sources.

In future studies, AMS users may consider utilizing a similar custom fit method (Section 3.5) to estimate the *RIE* of PMF-derived COA (as well as HOA or other factors) if high-quality instrument intercomparisons are available. In situations where intercomparisons cannot yield similar results (e.g., poor size distribution overlap between co-located instruments or saturation of an optical particle instrument), we recommend applying a $RIE_{COA}$ of 4.16 and *CE* of 1.0 to COA indoors and considering the applicability of a higher POA (HOA + COA) response factor (*RIE* × *CE* approximately 1.5 to 2) for outdoor datasets if POA is a large fraction of OA instead of using a $RIE_{OA}$ of 1.4 (and *CE* of 0.5) based on the re-analysis of prior studies (Docherty et al. 2011; Hayes et al. 2013; Jimenez et al. 2016; Avery, Waring, and DeCarlo 2019). The *RIE* of 4.16 is an average of the slope derived *RIE* from HOMEChem, ATHLETIC, and Reyes-Villegas et al. (2018). A graphical comparison of the *RIE* presented here and by Reyes-Villegas et al. (2018) is shown in Figure S20. Though there is some variability, the independently calibrated values from the three studies support that indoor $RIE_{COA}$ is higher than the value used for ambient organics (ambient $RIE_{OA} = 1.4$). Re-analysis of two ambient datasets (Hayes et al. 2013; Avery, Waring, and DeCarlo 2019) also indicated improved consistency between the AMS and co-located instruments when a higher response factor (*RIE* × *CE*) was applied to ambient PMF-derived POA (HOA + COA). The response factor for ambient POA does not appear to be as high as for fresh COA sampled indoors, but future studies of primary aerosol sources will be needed to quantify this effect. The reasons for increased detection efficiency of POA introduced by Jimenez et al. (2003) (electron ionization cross section) and theorized by Murphy (2016) (increased dwelling time in the detection region) may both play a role in the observed *RIE*, along with other effects.

As advanced instrumentation originally developed for studying ambient atmospheric chemistry is brought indoors, it is essential to consider possible response and quantification differences that may exist under the different sampling conditions. Indoors, aerosols emitted from a single source can reach high concentrations with limited evaporation and chemical aging and dominate observed concentrations for long periods of time, whereas outdoors, dilution, mixing, and chemical transformations play a much greater role in governing observed aerosol concentrations and composition. Atmospheric processing may alter the *RIE* or *CE* of fresh COA, possibly explaining why large discrepancies have not been widely noted. It is important to note that our goal is not always to reach 100% agreement with co-located instruments, as every instrument has specific biases in calculating particle concentration and associated uncertainty. Our aim is to highlight the improvement in AMS quantification methodology when a reduced primary source dominates the total observed particle concentration and further emphasize the importance of careful intercomparisons in future field studies.

## Funding

We acknowledge Paula Olsiewski and the Alfred P. Sloan Foundation for funding, including grant numbers G-2017-9944, 2019-12301, 2016-7173. HG, WLB, PCJ, DAD, and JLJ acknowledge the support from Sloan Foundation Grant No. G-2016-7173, and NASA Grant 80NSSC19K0124. JLJ, DAD, and WLB also thank a Cooperative Institute for Research in Environmental Sciences (CIRES) Innovative Research Program (IRP) grant, and a CIRES Fellowship for

WLB. AHG and DML acknowledge support from Sloan Foundation Grant No. G-2019-11412.

## ORCID

Erin F. Katz http://orcid.org/0000-0002-3726-1808
Hongyu Guo http://orcid.org/0000-0003-0487-3610
Pedro Campuzano-Jost http://orcid.org/0000-0003-3930-010X
Douglas A. Day http://orcid.org/0000-0003-3213-4233
Wyatt L. Brown http://orcid.org/0000-0003-3016-8958
Erin Boedicker http://orcid.org/0000-0002-4441-3312
Matson Pothier http://orcid.org/0000-0002-9526-1013
David M. Lunderberg http://orcid.org/0000-0002-4439-9194
Sameer Patel http://orcid.org/0000-0002-9293-9546
Kanan Patel http://orcid.org/0000-0002-2368-8624
Patrick L. Hayes http://orcid.org/0000-0002-6985-9601
Anita Avery http://orcid.org/0000-0002-6130-9664
Lea Hildebrandt Ruiz http://orcid.org/0000-0001-8378-1882
Allen H. Goldstein http://orcid.org/0000-0003-4014-4896
Marina E. Vance http://orcid.org/0000-0003-0940-0353
Delphine K. Farmer http://orcid.org/0000-0002-6470-9970
Jose L. Jimenez http://orcid.org/0000-0001-6203-1847
Peter F. DeCarlo http://orcid.org/0000-0001-6385-7149

## References

Abbatt, J. P. D., and C. Wang. 2020. The atmospheric chemistry of indoor environments. *Environ. Sci. Process. Impacts*. 22 (1):25–48. doi: 10.1039/c9em00386j.

Abdullahi, K. L., J. M. Delgado-Saborit, and R. M. Harrison. 2013. Emissions and indoor concentrations of particulate matter and its specific chemical components from cooking: A review. *Atmospheric Environ*. 71:260–94. doi: 10.1016/j.atmosenv.2013.01.061.

Aiken, A. C., B. de Foy, C. Wiedinmyer, P. F. DeCarlo, I. M. Ulbrich, M. N. Wehrli, S. Szidat, A. S. H. Prevot, J. Noda, L. Wacker, et al. 2010. Mexico City aerosol analysis during MILAGRO using high resolution aerosol mass spectrometry at the urban supersite (T0) – Part 2: Analysis of the biomass burning contribution and the non-fossil carbon fraction. *Atmospheric Chem. Phys.* 10 (12):5315–41. doi: 10.5194/acp-10-5315-2010.

Alfarra, M. R., H. Coe, J. D. Allan, K. N. Bower, H. Boudries, M. R. Canagaratna, J. L. Jimenez, J. T. Jayne, A. A. Garforth, S.-M. Li, et al. 2004. Characterization of urban and rural organic particulate in the Lower Fraser Valley using two aerodyne aerosol mass spectrometers. *Atmospheric Environ.* 38 (34):5745–58. doi: 10.1016/j.atmosenv.2004.01.054.

Allan, J. D., K. N. Bower, H. Coe, H. Boudries, J. T. Jayne, M. R. Canagaratna, D. B. Millet, A. H. Goldstein, P. K. Quinn, R. J. Weber, et al. 2004. Submicron aerosol composition at Trinidad Head, California, during ITCT 2K2: Its relationship with gas phase volatile organic carbon and assessment of instrument performance. *J. Geophys. Res. Atmos*. 109 (D23). doi: 10.1029/2003JD004208.

Allan, J. D., A. E. Delia, H. Coe, K. N. Bower, M. R. Alfarra, J. L. Jimenez, A. M. Middlebrook, F. Drewnick, T. B. Onasch, M. R. Canagaratna, et al. 2004. A generalized method for the extraction of chemically resolved mass spectra from Aerodyne aerosol mass spectrometer data. *J. Aerosol Sci.* 35 (7):909–22. doi: 10.1016/j.jaerosci.2004.02.007.

Allan, J. D., J. L. Jimenez, P. I. Williams, M. R. Alfarra, K. N. Bower, J. T. Jayne, H. Coe, and D. R. Worsnop. 2003. Quantitative sampling using an Aerodyne aerosol mass spectrometer - 1. Techniques of data interpretation and error analysis. *J. Geophys. Res. Atmos.* 108 (D3):10.

Avery, A. M., M. S. Waring, and P. F. DeCarlo. 2019. Seasonal variation in aerosol composition and concentration upon transport from the outdoor to indoor environment. *Environ. Sci: Process. Impacts* 21 (3):528–47. doi: 10.1039/C8EM00471D.

Bahreini, R., B. Ervens, A. M. Middlebrook, C. Warneke, J. A. d Gouw, P. F. DeCarlo, J. L. Jimenez, C. A. Brock, J. A. Neuman, T. B. Ryerson, et al. 2009. Organic aerosol formation in urban and industrial plumes near Houston and Dallas, TX. *J. Geophys. Res. Atmos.* 114. doi: 10.1029/2008JD011493.

Brown, W. L., D. A. Day, H. Stark, D. Pagonis, J. E. Krechmer, X. Liu, D. J. Price, E. F. Katz, P. F. DeCarlo, C. G. Masoud, et al. 2021. Real-time organic aerosol chemical speciation in the indoor environment using extractive electrospray ionization mass spectrometry. *Indoor Air*. 31 (1):141–55. doi: 10.1111/ina.12721.

Canagaratna, M. R., J. T. Jayne, J. L. Jimenez, J. D. Allan, M. R. Alfarra, Q. Zhang, T. B. Onasch, F. Drewnick, H. Coe, A. Middlebrook, et al. 2007. Chemical and microphysical characterization of ambient aerosols with the aerodyne aerosol mass spectrometer. *Mass Spectrom. Rev.* 26 (2):185–222. doi: 10.1002/mas.20115.

Canagaratna, M. R., J. L. Jimenez, J. H. Kroll, Q. Chen, S. H. Kessler, P. Massoli, L. Hildebrandt Ruiz, E. Fortner, L. R. Williams, K. R. Wilson, et al. 2015. Elemental ratio measurements of organic compounds using aerosol mass spectrometry: characterization, improved calibration, and implications. *Atmospheric Chem. Phys.* 15 (1):253–72. doi: 10.5194/acp-15-253-2015.

Crippa, M., I. E. Haddad, J. G. Slowik, P. F. DeCarlo, C. Mohr, M. F. Heringa, R. Chirico, N. Marchand, J. Sciare, U. Baltensperger, et al. 2013. Identification of marine and continental aerosol sources in Paris using high resolution aerosol mass spectrometry. *J. Geophys. Res. Atmos.* 118 (4):1950–63. doi: 10.1002/jgrd.50151.

Crounse, J. D., P. F. DeCarlo, D. R. Blake, L. K. Emmons, E. L. Campos, E. C. Apel, A. D. Clarke, A. J. Weinheimer, D. C. McCabe, R. J. Yokelson, et al. 2009. Biomass burning and urban air pollution over the central Mexican Plateau. *Atmospheric Chem. Phys.* 9 (14):4929–44. " doi: 10.5194/acp-9-4929-2009.

DeCarlo, P. F., J. R. Kimmel, A. Trimborn, M. J. Northway, J. T. Jayne, A. C. Aiken, M. Gonin, K. Fuhrer, T. Horvath, K. S. Docherty, et al. 2006. Field-Deployable. *Anal. Chem.* 78 (24):8281–9. doi: 10.1021/ac061249n.

DeCarlo, P. F., J. G. Slowik, D. R. Worsnop, P. Davidovits, and J. L. Jimenez. 2004. Particle morphology and density characterization by combined mobility and aerodynamic diameter

measurements. Part 1: Theory. *Aerosol Sci. Technol.* 38 (12): 1185–205. doi: 10.1080/027868290903907.

Docherty, K. S., A. C. Aiken, J. A. Huffman, I. M. Ulbrich, P. F. DeCarlo, D. Sueper, D. R. Worsnop, D. C. Snyder, R. E. Peltier, R. J. Weber, et al. 2011. The 2005 Study of organic aerosols at riverside (SOAR-1): Instrumental intercomparisons and fine particle composition. *Atmospheric Chem. Phys.* 11 (23):12387–420. doi: 10.5194/acp-11-12387-2011.

Dzepina, K., J. Arey, L. Marr, D. Worsnop, D. Salcedo, q Zhang, T. Onasch, L. Molina, M. Molina, and J. Jimenez. 2007. Detection of particle-phase polycyclic aromatic hydrocarbons in Mexico City using an aerosol mass spectrometer. *Int. J. Mass Spectrom.* 263 (2–3):152–70. doi: 10.1016/j.ijms.2007.01.010.

Farmer, D. K., M. E. Vance, J. P. D. Abbatt, A. Abeleira, M. R. Alves, C. Arata, E. Boedicker, S. Bourne, F. Cardoso-Sandaña, R. Corsi, et al. 2019. Overview of HOMEChem: House observations of microbial and environmental chemistry. *Environ. Sci: Process. Impacts* 21 (8): 1280–300. doi: 10.1039/C9EM00228F.

Finewax, Z., D. Pagonis, M. S. Claflin, A. V. Handschy, W. L. Brown, O. Jenk, B. A. Nault, D. A. Day, B. M. Lerner, J. L. Jimenez, et al. 2021. Quantification and source characterization of volatile organic compounds from exercising and application of chlorine-based cleaning products in a university athletic center. *Indoor Air*.

Guo, H., P. Campuzano-Jost, B. A. Nault, D. A. Day, J. C. Schroder, J. E. Dibb, M. Dollner, B. Weinzierl, and J. L. Jimenez. 2020. The importance of size ranges in aerosol instrument intercomparisons: A case study for the ATom Mission. *Atmos. Meas. Tech.* 2020:1–49.

Hayes, P. L., A. M. Ortega, M. J. Cubison, K. D. Froyd, Y. Zhao, S. S. Cliff, W. W. Hu, D. W. Toohey, J. H. Flynn, B. L. Lefer, et al. 2013. Organic aerosol composition and sources in Pasadena, California, during the 2010 CalNex campaign. *J. Geophys. Res. Atmos.* 118 (16):9233–57. doi: 10.1002/jgrd.50530.

Hering, S. V., S. R. Spielman, and G. S. Lewis. 2014. Moderated, water-based, condensational particle growth in a laminar flow. *Aerosol. Sci. Technol.* 48 (4):401–8. doi: 10.1080/02786826.2014.881460.

Hogrefe, O., J. J. Schwab, F. Drewnick, G. G. Lala, S. Peters, K. L. Demerjian, K. Rhoads, H. D. Felton, O. V. Rattigan, L. Husain, et al. 2004. Semicontinuous PM2.5 sulfate and nitrate measurements at an urban and a rural location in New York: PMTACS-NY Summer 2001 and 2002 Campaigns. *J. Air Waste Manag. Assoc.* 54 (9):1040–60. doi: 10.1080/10473289.2004.10470972.

Hu, W., P. Campuzano-Jost, D. A. Day, P. Croteau, M. R. Canagaratna, J. T. Jayne, D. R. Worsnop, and J. L. Jimenez. 2017. Evaluation of the new capture vaporizer for aerosol mass spectrometers (AMS) through field studies of inorganic species. *Aerosol Sci. Technol.* 51 (6): 735–54. doi: 10.1080/02786826.2017.1296104.

Hu, W., P. Campuzano-Jost, D. A. Day, P. Croteau, M. R. Canagaratna, J. T. Jayne, D. R. Worsnop, and J. L. Jimenez. 2017. Evaluation of the new capture vapourizer for aerosol mass spectrometers (AMS) through laboratory studies of inorganic species. *Atmos. Meas. Tech.* 10 (8): 2897–921. doi: 10.5194/amt-10-2897-2017.

Hu, W., P. Campuzano-Jost, D. A. Day, B. A. Nault, T. Park, T. Lee, A. Pajunoja, A. Virtanen, P. Croteau, M. R. Canagaratna, et al. 2020. Ambient quantification and size distributions for organic aerosol in aerosol mass spectrometers with the new capture vaporizer. *ACS Earth Space Chem.* 4 (5):676–89. doi: 10.1021/acsearthspacechem.9b00310.

Huffman, J. A., J. T. Jayne, F. Drewnick, A. C. Aiken, T. Onasch, D. R. Worsnop, and J. L. Jimenez. 2005. Design, modeling, optimization, and experimental tests of a particle beam width probe for the Aerodyne aerosol mass spectrometer. *Aerosol Sci. Technol.* 39 (12):1143–63. doi: 10.1080/02786820500423782.

Ide, Y., K. Uchida, and N. Takegawa. 2019. Ionization efficiency of evolved gas molecules from aerosol particles in a thermal desorption aerosol mass spectrometer: Numerical simulations. *Aerosol Sci. Technol.* 53 (7): 843–52. doi: 10.1080/02786826.2019.1612512.

Jimenez, J. L., M. R. Canagaratna, F. Drewnick, J. D. Allan, M. R. Alfarra, A. M. Middlebrook, J. G. Slowik, Q. Zhang, H. Coe, J. T. Jayne, et al. 2016. Comment on "The effects of molecular weight and thermal decomposition on the sensitivity of a thermal desorption aerosol mass spectrometer". *Aerosol Sci. Technol.* 50 (9):i–xv. doi: 10.1080/02786826.2016.1205728.

Jimenez, J. L., J. T. Jayne, Q. Shi, C. E. Kolb, D. R. Worsnop, I. Yourshaw, J. H. Seinfeld, R. C. Flagan, X. F. Zhang, K. A. Smith, et al. 2003. Ambient aerosol sampling using the Aerodyne Aerosol Mass Spectrometer. *J. Geophys. Res. Atmos.* 108 (D7):13. doi: 10.1029/2001JD001213.

Kim, H., Q. Zhang, and J. Heo. 2018. Influence of intense secondary aerosol formation and long-range transport on aerosol chemistry and properties in the Seoul Metropolitan Area during spring time: results from KORUS-AQ. *Atmos. Chem. Phys.* 18 (10):7149–68. doi: 10.5194/acp-18-7149-2018.

Klepeis, N. E., W. C. Nelson, W. R. Ott, J. P. Robinson, A. M. Tsang, P. Switzer, J. V. Behar, S. C. Hern, and W. H. Engelmann. 2001. The National Human Activity Pattern Survey (NHAPS): A resource for assessing exposure to environmental pollutants. *J. Expo. Sci. Environ. Epidemiol.* 11 (3):231–52. doi: 10.1038/sj.jea.7500165.

Knote, C., D. Brunner, H. Vogel, J. Allan, A. Asmi, M. Äijälä, S. Carbone, H. D. van der Gon, J. L. Jimenez, A. Kiendler-Scharr, et al. 2011. Towards an online-coupled chemistry-climate model: evaluation of trace gases and aerosols in COSMO-ART. *Geosci. Model Dev.* 4 (4): 1077–102. doi: 10.5194/gmd-4-1077-2011.

Kuwata, M., S. R. Zorn, and S. T. Martin. 2012. Using elemental ratios to predict the density of organic material composed of carbon, hydrogen, and oxygen. *Environ. Sci. Technol.* 46 (2):787–94. doi: 10.1021/es202525q.

Lanz, V. A., M. R. Alfarra, U. Baltensperger, B. Buchmann, C. Hueglin, and A. S. H. Prévôt. 2007. Source apportionment of submicron organic aerosols at an urban site by factor analytical modelling of aerosol mass spectra. *Atmospheric Chem. Phys.* 7 (6):1503–22. doi: 10.5194/acp-7-1503-2007.

Liu, T. Y., Z. Y. Wang, X. M. Wang, and C. K. Chan. 2018. Primary and secondary organic aerosol from heated cooking oil emissions. *Atmospheric Chem. Phys.* 18 (15): 11363–74. doi: 10.5194/acp-18-11363-2018.

Lunderberg, D. M., K. Kristensen, Y. Tian, C. Arata, P. K. Misztal, Y. Liu, N. Kreisberg, E. F. Katz, P. F. DeCarlo, S. Patel, et al. 2020. Surface emissions modulate indoor SVOC concentrations through volatility-dependent

partitioning. *Environ. Sci. Technol.* 54 (11):6751–60. doi: 10.1021/acs.est.0c00966.

Matthew, B. M., A. M. Middlebrook, and T. B. Onasch. 2008. Collection efficiencies in an Aerodyne aerosol mass spectrometer as a function of particle phase for laboratory generated aerosols. *Aerosol Sci. Technol.* 42 (11): 884–98. doi: 10.1080/02786820802356797.

Middlebrook, A. M., R. Bahreini, J. L. Jimenez, and M. R. Canagaratna. 2012. Evaluation of composition-dependent collection efficiencies for the aerodyne aerosol mass spectrometer using field data. *Aerosol Sci. Technol.* 46 (3): 258–71. doi: 10.1080/02786826.2011.620041.

Minguillón, M. C., A. Ripoll, N. Pérez, A. S. H. Prévôt, F. Canonaco, X. Querol, and A. Alastuey. 2015. Chemical characterization of submicron regional background aerosols in the western Mediterranean using an Aerosol Chemical Speciation Monitor. *Atmospheric Chem. Phys.* 15 (11):6379–91. doi: 10.5194/acp-15-6379-2015.

Mohr, C., P. F. DeCarlo, M. F. Heringa, R. Chirico, J. G. Slowik, R. Richter, C. Reche, A. Alastuey, X. Querol, R. Seco, et al. 2012. Identification and quantification of organic aerosol from cooking and other sources in Barcelona using aerosol mass spectrometer data. *Atmospheric Chem. Phys.* 12 (4):1649–65. doi: 10.5194/acp-12-1649-2012.

Mohr, C., J. A. Huffman, M. J. Cubison, A. C. Aiken, K. S. Docherty, J. R. Kimmel, I. M. Ulbrich, M. Hannigan, and J. L. Jimenez. 2009. Characterization of primary organic aerosol emissions from meat cooking, trash burning, and motor vehicles with high-resolution aerosol mass spectrometry and comparison with ambient and chamber observations. *Environ. Sci. Technol.* 43 (7):2443–9. doi: 10.1021/es8011518.

Murphy, D. M. 2016. The effects of molecular weight and thermal decomposition on the sensitivity of a thermal desorption aerosol mass spectrometer. *Aerosol Sci. Technol.* 50 (2):118–25. doi: 10.1080/02786826.2015.1136403.

Nault, B. A., P. Campuzano-Jost, D. A. Day, J. C. Schroder, B. Anderson, A. J. Beyersdorf, D. R. Blake, W. H. Brune, Y. Choi, C. A. Corr, et al. 2018. Secondary organic aerosol production from local emissions dominates the organic aerosol budget over Seoul, South Korea, during KORUS-AQ. *Atmospheric Chem. Phys.* 18 (24): 17769–800. doi: 10.5194/acp-18-17769-2018.

Nazaroff, W. W., and A. H. Goldstein. 2015. Indoor chemistry: research opportunities and challenges. *Indoor Air.* 25 (4):357–61. doi: 10.1111/ina.12219.

Ng, N. L., S. C. Herndon, A. Trimborn, M. R. Canagaratna, P. L. Croteau, T. B. Onasch, D. Sueper, D. R. Worsnop, Q. Zhang, Y. L. Sun, et al. 2011. An Aerosol Chemical Speciation Monitor (ACSM) for routine monitoring of the composition and mass concentrations of ambient aerosol. *Aerosol Sci. Technol.* 45 (7):780–94. doi: 10.1080/02786826.2011.560211.

Park, K., D. B. Kittelson, M. R. Zachariah, and P. H. McMurry. 2004. Measurement of inherent material density of nanoparticle agglomerates. *J. Nanopart. Res.* 6 (2/3):267–72. doi: 10.1023/B:NANO.0000034657.71309.e6.

Patel, S., S. Sankhyan, E. K. Boedicker, P. F. DeCarlo, D. K. Farmer, A. H. Goldstein, E. F. Katz, W. W. Nazaroff, Y. Tian, J. Vanhanen, et al. 2020. Indoor particulate matter during HOMEChem: Concentrations, size distributions, and exposures. *Environ. Sci. Technol.* 54 (12):7107–16. doi: 10.1021/acs.est.0c00740.

Reyes-Villegas, E., T. Bannan, M. L. Breton, A. Mehra, M. Priestley, C. Percival, H. Coe, and J. D. Allan. 2018. Online chemical characterization of food-cooking organic aerosols: Implications for source apportionment. *Environ. Sci. Technol.* 52 (9):5308–18. doi: 10.1021/acs.est.7b06278.

Robinson, E. S., P. Gu, Q. Ye, H. Z. Li, R. U. Shah, J. S. Apte, A. L. Robinson, and A. A. Presto. 2018. Restaurant impacts on outdoor air quality: Elevated organic aerosol mass from restaurant cooking with neighborhood-scale plume extents. *Environ. Sci. Technol.* 52 (16):9285–94. doi: 10.1021/acs.est.8b02654.

Robinson, E. S., T. B. Onasch, D. Worsnop, and N. M. Donahue. 2017. Collection efficiency of α-pinene secondary organic aerosol particles explored via light-scattering single-particle aerosol mass spectrometry. *Atmos. Meas. Tech.* 10 (3):1139–54. doi: 10.5194/amt-10-1139-2017.

Salcedo, D., T. B. Onasch, K. Dzepina, M. R. Canagaratna, Q. Zhang, J. A. Huffman, P. F. Decarlo, J. T. Jayne, P. Mortimer, D. R. Worsnop, et al. 2006. Characterization of ambient aerosols in Mexico City during the MCMA-2003 campaign with Aerosol Mass Spectrometry: results from the CENICA Supersite. *Atmospheric Chem. Phys.* 6 (4):925–46. doi: 10.5194/acp-6-925-2006.

Schroder, J. C., P. Campuzano-Jost, D. A. Day, V. Shah, K. Larson, J. M. Sommers, A. P. Sullivan, T. Campos, J. M. Reeves, A. Hills, et al. 2018. Sources and secondary production of organic aerosols in the Northeastern United States during WINTER. *J. Geophys. Res. Atmos.* 123(14):7771–96.

Sloane, C. S., J. Watson, J. Chow, L. Pritchett, and L. W. Richards. 1991. Size-segregated fine particle measurements by chemical species and their impact on visibility impairment in Denver. *Atmos. Environ. Part A.* 25 (5–6): 1013–24. doi: 10.1016/0960-1686(91)90143-U.

Slowik, J. G., K. Stainken, P. Davidovits, L. R. Williams, J. T. Jayne, C. E. Kolb, D. R. Worsnop, Y. Rudich, P. F. DeCarlo, and J. L. Jimenez. 2004. Particle morphology and density characterization by combined mobility and aerodynamic diameter measurements. Part 2: Application to combustion-generated soot aerosols as a function of fuel equivalence ratio. *Aerosol Sci. Technol.* 38 (12): 1206–22. doi: 10.1080/027868290903916.

Stein, S. W., B. J. Turpin, X. Cai, P.-F. Huang, and P. H. McMurry. 1994. Measurements of relative humidity-dependent bounce and density for atmospheric particles using the DMA-impactor technique. *Atmospheric Environ.* 28 (10):1739–46. doi: 10.1016/1352-2310(94)90136-8.

Uchida, K., Y. Ide, and N. Takegawa. 2019. Ionization efficiency of evolved gas molecules from aerosol particles in a thermal desorption aerosol mass spectrometer: Laboratory experiments. *Aerosol Sci. Technol.* 53 (1): 86–93. doi: 10.1080/02786826.2018.1544704.

Ulbrich, I. M., M. R. Canagaratna, Q. Zhang, D. R. Worsnop, and J. L. Jimenez. 2009. Interpretation of organic components from positive matrix factorization of aerosol mass spectrometric data. *Atmospheric Chem. Phys.* 9 (9):2891–918. doi: 10.5194/acp-9-2891-2009.

Xu, W., A. Lambe, P. Silva, W. Hu, T. Onasch, L. Williams, P. Croteau, X. Zhang, L. Renbaum-Wolff, E. Fortner,

et al. 2018. Laboratory evaluation of species-dependent relative ionization efficiencies in the aerodyne aerosol mass spectrometer. *Aerosol Sci. Technol.* 52 (6):626–41. doi: 10.1080/02786826.2018.1439570.

Yin, J., S. A. Cumberland, R. M. Harrison, J. Allan, D. E. Young, P. I. Williams, and H. Coe. 2015. Receptor modelling of fine particles in southern England using CMB including comparison with AMS-PMF factors. *Atmospheric Chem. Phys.* 15 (4):2139–58. doi: 10.5194/acp-15-2139-2015.

Zhang, Q., J. L. Jimenez, M. R. Canagaratna, J. D. Allan, H. Coe, I. Ulbrich, M. R. Alfarra, A. Takami, A. M. Middlebrook, Y. L. Sun, et al. 2007. Ubiquity and dominance of oxygenated species in organic aerosols in anthropogenically-influenced Northern Hemisphere midlatitudes. *Geophys. Res. Lett.* 34 (13). doi: 10.1029/2007GL029979.